Biogeosciences Discuss., 9, 9201–9231, 2012
www.biogeosciences-discuss.net/9/9201/2012/
doi:10.5194/bgd-9-9201-2012

Biogeosciences Discussions

Sediment-water column fluxes of carbon, oxygen and nutrients in Bedford Basin, Nova Scotia, inferred from ^{224}Ra measurements

W. J. Burt[1], H. Thomas[1], K. Fennel[1], and E. Horne[2]

[1]Dalhousie University, Department of Oceanography, Halifax, NS, Canada
[2]Bedford Institute of Oceanography, Fisheries & Oceans Canada, Dartmouth, NS, Canada

Received: 15 June 2012 – Accepted: 4 July 2012 – Published: 24 July 2012

Correspondence to: W. J. Burt (willburt@dal.ca)

Published by Copernicus Publications on behalf of the European Geosciences Union.

Abstract

Exchanges between sediment pore waters and the overlying water column play a significant role in the chemical budgets of many important chemical constituents. Quantification of such benthic fluxes requires explicit knowledge of the sediment properties and biogeochemistry. Alternatively, changes in water column properties near the sediment-water column interface can be exploited to gain insight into the sediment biogeochemistry and benthic fluxes. Here, we apply a 1-D diffusive mixing model to near-bottom water column profiles of ^{224}Ra activity in order to yield vertical eddy diffusivities (K_Z), based upon which we assess the diffusive exchange of inorganic carbon (DIC), nutrients and oxygen (O_2), across the sediment-water interface in a coastal inlet, Bedford Basin, Nova Scotia, Canada. Near-bottom observations of DIC, O_2 and nutrients provide flux ratios similar to Redfield values, suggesting that benthic respiration of primarily marine organic matter is the dominant driver. Furthermore, we did not observe any significant release of alkalinity (A_T) from the sediments to the overlying water column, providing further insight into the dominant reactions taking place within sediments: the respiration of organic matter occurs largely under aerobic conditions or products of anaerobic processes are reoxidized quickly in oxygenated layers of the sediments. Finally, comparison with other carbon sources reveal the observed benthic DIC release as a significant contributor to the Bedford Basin carbon system.

1 Introduction

A fraction of the particulate organic matter (POM) generated photosynthetically in the euphotic zone settles to the sediment where microbes utilize a variety of electron acceptors to respire this organic material producing dissolved inorganic carbon (DIC) and nutrients. As a result, sediment pore waters become highly concentrated in many chemical constituents relative to the overlying water column (Moore et al., 2011; Charette et al., 2007) so that small volumes of discharged fluid can have

BGD
9, 9201–9231, 2012

disproportionately large affects on biogeochemical cycles and budgets (Berelson et al., 1987). Furthermore, if considering the area over which these processes can occur, from smaller basins to entire continental margins, fluxes from sediments can be a major source or sink in various coastal chemical budgets (Fennel et al., 2006). For example, in the shallow mud flats of the North Sea, anaerobic alkalinity generation within the sediments, and its subsequent release, may facilitate up to 25 % of the North Sea CO_2 uptake (Thomas et al., 2009). Pore water fluxes in the shallow Wadden Sea have been shown to largely control the budgets of numerous important chemical constituents, including alkalinity, silica, manganese and uranium (Moore et al., 2011). Consequently, many studies have focused on quantifying the release of pore waters in coastal environments (Colbert and Hammond, 2008; Jahnke and Jahnke, 2000; Hancock et al., 2006; Simmons Jr., 1992), and modelling the biogeochemistry of chemical fluxes across the sediment-water interface (Fennel et al., 2009). While the relative magnitude of the benthic fluxes can vary greatly over regional scales, balancing of biogeochemical budgets in oceanic environments requires the consideration of sediment-water column interactions.

Pore waters enter the water column via a number of different physical processes, many of which occur at slow rates, making their detection and quantification difficult (Burnett et al., 2003). However, if we assume that fluxes across the sediment-water interface are controlled by diffusive processes, such fluxes out of the pore water into the overlying water column can be inferred using the short-lived radioactive tracer, ^{224}Radium (^{224}Ra), a powerful tool commonly used for estimating various types of submarine groundwater discharge (SGD) fluxes. Due to its high affinity for sediment surfaces, ^{228}Thorium (^{228}Th), the longer-lived parent isotope of ^{224}Ra, is ever present within bottom sediments. Consequently, ^{224}Ra, which has a much lower affinity for sediment surfaces, is constantly produced and becomes highly concentrated in the interstitial pore water. As this ^{224}Ra diffuses into the overlying water column, ^{224}Ra is mixed away from its source, and its activity decreases. Utilizing the decay timescales of ^{224}Ra

BGD
9, 9201–9231, 2012

($t_{1/2}$ = 3.66 d), diffusion rates near the seafloor can be estimated and subsequently applied to chemical gradients of other dissolved constituents.

Sediment-water column exchange of carbon and nutrients is often quantified using in situ benthic flux chambers (Berelson et al., 1987; Jahnke et al., 2000; Jahnke and Jahnke, 2000). Alternatively, benthic fluxes can be estimated by measuring pore water profiles of nutrients or metals (Emerson et al., 1984; Jahnke et al., 2005; Lettmann et al., 2012) or more recently, radium isotopes (Hancock et al., 2006; Colbert and Hammond, 2008; Moore et al., 2011) and applying models to the resulting gradients. Modelling pore water data, however, requires a thorough understanding of various sediment qualities (i.e. composition, porosity, density), which often involve intricate lab experiments using sediment cores and can result in highly uncertain estimates, especially when dealing with permeable sediments (Huettel and Webster, 2001).

In this study, a more direct observational approach is applied to measure the fluxes of ^{224}Ra, DIC and dissolved oxygen (O_2) between the sediments and water column that relies on water column observations. Specifically, we estimated the vertical diffusive flux of the short-lived ^{224}Ra from the seafloor into the bottom water in Bedford Basin (Halifax Harbour, NS). Then, we apply a 1-D diffusion model to near-bottom vertical profiles of ^{224}Ra to asses both the vertical eddy diffusivity in the water column (K_Z), and the ^{224}Ra activity at the sediment surface (A_0). These calculated values, along with estimates of the benthic flux of ^{224}Ra per unit area of seafloor, are compared to other published values from similar studies. Near-bottom gradients of DIC and O_2 are then used in conjunction with the estimates of K_Z to quantify the diffusive release of carbon into the water column and corresponding uptake of O_2 by the sediments. Further, estimates of nutrient (nitrate and phosphate) fluxes are also made using time-series observations at the bottom of the basin. By contrasting the inferred carbon flux with estimates of both riverine DIC input and uptake by primary production, the relative contribution of the benthic flux to the carbon budget in Bedford Basin is established.

BGD
9, 9201–9231, 2012

2 Methods

2.1 Study site

Observations were made between October and December of 2010 at the Compass Buoy station in Bedford Basin, Nova Scotia, Canada (44° 41′ 30″ N, 63° 38′ 30″ W). Bedford Basin is a small enclosed bay (6 km long by 4 km wide) at the northwestern end of Halifax Harbour (Fig. 1). The Basin reaches water depths of over 70 m, while the rest of Halifax Harbour is relatively shallow (Fig. 1). The only major fresh water source in the region, the Sackville River, drains into the northwestern side of Bedford Basin with an approximate annual discharge of 1.5×10^8 m^3 yr^{-1} (Kepkay et al., 1997). At the southeastern edge, water exits into the Narrows, eventually leading to the Halifax Outer Harbour and the Scotian Shelf.

The general circulation pattern of Halifax Harbour is described as a two-layer estuarine type circulation with a relatively fresh upper layer moving seaward driven by inputs from the Sackville River and a saltier deep-water return flow (Fader and Millar, 2008). However, this circulation is at its weakest in Bedford Basin, with a mean surface outflow of 0.2 cm s^{-1}. Also, the entrance to the Narrows is marked by a shallow sill with a depth of about 20 m, and while significant tidal currents can be observed within the Narrows, the presence of the sill largely prevents mixing below 20–30 m depth in the Basin (Shan et al., 2011). As a result, and as seen in the homogenous temperature and salinity distributions (Fig. 2), the subsurface layers of Bedford Basin are a relatively stable environment, which, for the purpose of this study, allows us to apply the 1-D diffusive model described below. However, periodic storms in the spring and fall can result in deep water ventilation events, one of which occurred in October 2010 and terminated toward the start of the sampling period (Figs. 2–4). These events can result from wind-induced deep vertical mixing during periods of minimum stratification (Punshon and Moore, 2004). However, the October 2010 event is more likely to have resulted via lateral intrusion, the mechanism for which is described as a combination of strong along-shore winds and large tides, causing a build-up of coastal sea level and

BGD
9, 9201–9231, 2012

bringing dense water from the outer harbour over the sill and into the deep basin (Platt et al., 1972). Regardless of the specific mechanism for their occurrence, these events result in abrupt changes in the physical and chemical characteristics of the deep water column (Fig. 2), bringing surface waters saturated with oxygen into the deep basin and preventing the deep waters from reaching anoxic conditions (Fig. 3) (Hargrave et al., 1976). Concurrently, deep waters, rich in dissolved carbon and nutrients, are brought to the surface, occasionally marking the onset of the spring or autumn phytoplankton bloom (Fig. 3).

The close proximity of Bedford Basin to both the Bedford Institute of Oceanography (BIO) and Dalhousie University allow for convenient access for weekly measurements. The Bedford Basin Plankton Monitoring Program conducted at BIO has been taking weekly measurements of various water properties, including nutrient levels, plankton records, and CTD profiles at the Compass Buoy site for nearly 30 yr (Li and Dickie, 2001). Also, the lack of significant horizontal or vertical advective flows in the deep waters of Bedford Basin allows for a reliable application of the assumptions necessary for the 1-D diffusion model utilized in this study.

2.2 Vertical mixing coefficients derived from radium tracers

The method for quantifying turbulent diffusion near the sediment surface is based on the 1-dimensional model used in conjunction with short-lived radium by Moore (2000), and subsequently applied in various settings (Moore, 2003; Charette et al., 2007; Men et al., 2011; Moore and Oliveira, 2008). The original model quantified the diffusive flux of short-lived radium isotopes in the horizontal direction from a point source (i.e. the coast) towards the open ocean. The model used here takes the same basic concepts used in the Moore (2000) model, and applies them in the vertical direction, similar to the approach taken in the deep Southern Ocean by Charette et al. (2007), describing the vertical transport of ^{224}Ra, via turbulent diffusion, from its source on the sediment surface.

BGD
9, 9201–9231, 2012

Assuming that the activity distribution of the radioactive tracer radium (A) in the water column is controlled by inputs, transport and radioactive decay (with decay constant λ), the change in radium activity over time ($\mathrm{d}A/\mathrm{d}t$) is described using a general diffusion equation with an additional decay term,

$$\frac{\mathrm{d}A}{\mathrm{d}t} = K_Z \frac{\partial^2 A}{\partial z^2} - \lambda A. \quad (1)$$

Here, z represents the vertical distance from the sediment surface. The 1-D diffusion model is applied in the vertical direction and assumed to have a single constant source of radium, with activity A, at the lower boundary representing the sediment surface ($z = 0$). Radium is mixed away from the surface by turbulent diffusion at a constant rate K_Z. The activity will drop to 0 at some distance from the source ($A \to 0$ as $z \to \infty$). Assuming steady-state, the vertical distribution of A is described by:

$$A(z) = A_0 \mathrm{e}^{\left[-z\sqrt{\lambda/K_Z}\right]}, \quad (2)$$

where $A(z)$ is the ^{224}Ra activity at depth z. Taking the natural log of Eq. (2) yields a linear equation of the ln of activity over depth, i.e.,

$$\ln(A(z)) = \ln(A_0) - z\sqrt{\lambda/K_Z}, \quad (3)$$

from which the slope ($-\sqrt{\lambda/K_Z}$) and intercept ($\ln(A_0)$) can be obtained by linear least-squares regression. The vertical eddy diffusion coefficient (K_Z) can then be determined from the slope using knowledge of the ^{224}Ra decay constant ($\lambda = 0.19\,\mathrm{day}^{-1}$).

2.3 Calculating benthic radium, carbon, oxygen, and nutrient fluxes

By obtaining estimates of eddy diffusivity and interface activity, one can calculate the flux of radium from a unit area of seafloor into the overlying water column. Integrating

BGD
9, 9201–9231, 2012

Eq. (2) over z from 0 to ∞ yields:

$$Q_{\mathrm{Ra}} = A_0 \sqrt{\frac{K_Z}{\lambda}}, \tag{4}$$

where Q_{Ra} is the benthic radium flux (atoms Ra $\mathrm{m}^{-2}\,\mathrm{s}^{-1}$).

Next, according to Fick's first law, combining the vertical concentration gradients ($[\mathrm{mmol\,m}^{-3}]\,\mathrm{m}^{-1}$) in carbon ($\mathrm{dDIC}/\mathrm{d}z$) and oxygen ($\mathrm{d}O_2/\mathrm{d}z$), with the Ra-derived eddy diffusivities, the vertical fluxes of carbon and oxygen per square meter of sediment surface ($\mathrm{mmol\,m}^{-2}\,\mathrm{d}^{-1}$), can be computed for each sampling day:

$$Q_{\mathrm{DIC}} = -K_Z \left[\frac{\mathrm{dDIC}}{\mathrm{d}z}\right] \tag{5}$$

$$Q_{\mathrm{O_2}} = -K_Z \left[\frac{\mathrm{dO_2}}{\mathrm{d}z}\right] \tag{6}$$

Assuming negligible respiration within the deep water column, the ratios of the concentration changes of NO_3^- ($m_{NO_3^-}$) vs. O_2 (m_{O_2}) and PO_4^{3-} (m_{PO_4}) vs. O_2 were applied to the oxygen flux (Q_{O_2}) in order to calculate the benthic nutrient fluxes, Q_{NO_3} and Q_{PO_4} ($\mathrm{mmol\,m}^{-2}\,\mathrm{d}^{-1}$), respectively:

$$Q_{NO_3^-} = Q_{O_2} \frac{m_{NO_3^-}}{m_{O_2}} \tag{7}$$

$$Q_{PO_4^{3-}} = Q_{O_2} \frac{m_{PO_4^{3-}}}{m_{O_2}} \tag{8}$$

The uncertainties are reported for the majority of the values calculated in this analysis using the standard error propagation formula for uncorrelated variables. First, the uncertainty for each individual parameter (i.e. ^{224}Ra, DIC) is determined. These values

BGD
9, 9201–9231, 2012

are then applied to the linear fits using a weighted least-squares regression, which fits the data while taking into account the uncertainties and provides a separate uncertainty in the resulting slope and intercept coefficients.

2.4 Analytical methods

Samples of ^{223}Ra and ^{224}Ra were taken aboard the vessel CCGS Sigma T, operated out of the Bedford Institute of Oceanography. In total, five vertical profiles of ^{224}Ra were sampled between October and December of 2010. Each sample requires a large volume of water (150–200 l) which was obtained at the surface (~2 m) using a small bilge pump that was lowered over the side of the vessel, and at depth using repeated casts of 30 l Niskin bottles lowered to the appropriate depths. Once collected, sample volumes were pumped through 10 and 1 µm cartridge filters to remove any particles, effectively removing all sources of the parent ^{228}Th isotopes. The water was then passed slowly ($< 1\,\mathrm{l\,min^{-1}}$) through plastic cartridges packed with 20 g of pre-weighed MnO_2-impregnated fiber, which quantitatively extracts the radium isotopes (Moore, 1987). The fibers were then rinsed with de-ionized water and dried to a water/fiber ratio between 0.3–1.1 using compressed air to maximize the emanation of radon (Rn) from the fibers during counting (Sun and Torgersen, 1998).

In order to analyze ^{224}Ra activities of samples, the cartridges were placed onto the RaDeCC coincidence counting system described by Moore and Arnold (1996). Using the electronic time windows within a photomultiplier tube (PMT), the instrument is able to identify and distinguish between the alpha particles created by the decay of ^{223}Ra and ^{224}Ra as well as their respective daughters, $^{219/220}$Rn. To minimize initial decay, all samples were counted within 2 days of collection. The samples were then aged for approximately 3 weeks, allowing all excess ^{224}Ra to equilibrate with parent ^{228}Th before recounting to calculate the initial supported Ra. The uncertainty in the ^{224}Ra measurements ranged between 7–10 %.

The majority of the radium samples were also accompanied by bottle samples of dissolved inorganic carbon (DIC) and alkalinity (A_T). These samples were collected

BGD
9, 9201–9231, 2012

and poisoned with a $HgCl_2$ solution to halt biological activity, before being stored for later analysis by coulometric determination on the VINDTA 3C (Versatile Instrument for the Determination of Titration Alkalinity by Marianda) (see Johnson et al., 1993 for a full description of instrumental methods).

Vertical profiles of temperature, conductivity, and pressure were collected using a seabird SBE25 CTD profiler, equipped with a Beckman/YSI type dissolved oxygen sensor. Additionally, discrete bottle samples (at 1, 5, 10, 60 m depth) were taken by Niskin bottle and analyzed for various biological and chemical species as part of the Bedford Basin Monitoring Program, providing time-series data of oxygen, nitrate (NO_3^-), phosphate (PO_4^{3-}), chlorophyll (chl *a*) and particulate organic carbon (POC) during the sampling period. This additional sampling always took place within 1 day of radium sampling.

3 Results

3.1 Radium distribution

The vertical ^{224}Ra distributions during the sampling period (Fig. 5) show relatively small activities in shallow and intermediate waters, with relatively large enrichments near the sediment surface. The ^{224}Ra signal in the upper 10 m of the water column can be attributed to the Sackville river, which discharges Ra-rich freshwater a few kilometres northeast of the sampling site. Variability in river discharge and the flushing effect of the daily tidal cycle may explain the weekly variability between surface and shallow (10 m) samples.

Focusing on deeper samples (Fig. 5b), significant ^{224}Ra enrichment was observed near the sediment surface in all 5 profiles, indicating a source of ^{224}Ra from the seafloor, similar to water-column observations in the deep Southern Ocean (Charette et al., 2007) and pore water results in many coastal environments (Hancock et al., 2006; Colbert and Hammond, 2008; Moore et al., 2011). Due to the isotope's short

BGD
9, 9201–9231, 2012

half-life ($t_{1/2}$ = 3.66 d) and the quiescent nature of Bedford Basin's deep water, we observed a decrease in radium activity over a relatively short distance away from the sediments.

Application of the 1-D diffusive model, illustrated in Fig. 5b, yields K_Z values ranging from 1.0–3.3 $cm^2 s^{-1}$, with uncertainties ranging from 25–30 %, with the exception of the 26 October profile, which yields a value of 25.7 $cm^2 s^{-1}$ with uncertainties near 100 % (Table 1). The single outlier on 26 October was attributed to additional advective forces from a lateral intrusion event, violating the zero-advection assumption of the 1-D diffusive model. Therefore, the data were not used in further analysis (see discussion). In general, however, the observed diffusivity decreases throughout the sampling period. These observed diffusivities fall within the lower end of the range of values (1–100 $cm^2 s^{-1}$) obtained during an extensive dye tracing experiment in coastal and estuarine waters around the UK (Riddle and Lewis, 2000). This is not surprising given the relatively quiescent nature of the deep waters of Bedford Basin. Although no prior estimates are available for Bedford Basin, similar models in other regions have produced similar K_Z values. Charette et al. (2007) used the longer lived ^{228}Ra isotope in a similar diffusion model to calculate a K_Z of 1.5 $cm^2 s^{-1}$ in the intermediate waters (300–1000 m) of the Southern Ocean. Berelson et al. (1982) used ^{222}Rn in the 500 m deep Santa Barbara basin to calculate a vertical diffusivity of 3.4 $cm^2 s^{-1}$, but also reported that near-bottom mixing created difficulties in fitting the 1-dimensional model.

3.2 ^{224}Ra, DIC, O_2 and nutrient fluxes

Using the intercept values from Fig. 5b, the interpolated radium activity at the sediment surface (A_0) also shows a general increase over time, ranging from 11.9–31.6 dpm 100 l^{-1} with uncertainties ranging from 19–27 %. Utilizing these estimates of daily A_0 along with the K_Z values, we obtained daily radium fluxes (Q_{Ra}) that show a general increase throughout the sampling period, and range from 24.4–36.9 atoms Ra $m^{-2} s^{-1}$. Uncertainties on this term varied significantly and in some cases were high (17–171 %)

BGD
9, 9201–9231, 2012

due to the cubic relationship of the slope term in the error propagation formula. These results are summarized in Table 1. For comparison, Colbert and Hammond (2008) collected sediment cores in San Pedro Bay, CA, and using pore water ^{224}Ra profiles and incubation experiments, obtained a radium flux of 32.4 atoms Ra m^{-2} s^{-1}. The authors describe their benthic flux as a combination of molecular diffusion (10 %), and non-local exchange (90 %), where within the sediments, parcels of pore water exchange with overlying parcels at a given rate. Berelson et al. (1982) used ^{222}Rn in the same 1-D model, and reported standing crops of 53 and 376 atoms Rn m^{-2} s^{-1} for two separate basins. The fact that these previously published results are similar to the ones reported here provides support for the approach of creating benthic radium flux estimates using only water column measurements. However, caution must be taken when directly comparing the observed results to those found in other regions, due to variations in numerous important factors (e.g. sediment cover, methodology).

The overall trends seen in the vertical distributions of DIC and O_2 in Bedford Basin (Fig. 6b, c) mimic those seen in the radium observations, with clear vertical gradients near the sediment surface. No visible gradients, however, are seen in the deep-water A_T data (Fig. 6a). The DIC gradient also becomes increasingly negative throughout the study period (i.e. concentration decreases with distance from the sediments, see Fig. 6), while the opposing O_2 gradient generally becomes increasingly positive. The vertical gradients in both DIC (Fig. 6d) and O_2 (Fig. 6e) were quantified for each sampling day using a weighted least-squares regression of all data over the same depth ranges. The interpolation of the DIC linear regressions to the sediment surface yield a wide range of interface concentrations (2199–2336 µmol l^{-1}), and like the individual radium interface activities, the values increase considerably throughout the sampling period.

While estimates of K_Z were made weekly throughout the sampling period, and weekly O_2 profiles are consistently available from the Bedford Basin Monitoring Program, the DIC and O_2 fluxes were calculated only for days where both DIC and ^{224}Ra observations were made. As seen in Table 1, both fluxes strengthen, with opposing

BGD
9, 9201–9231, 2012

signs, throughout the majority of the sampling period. Assuming the changes in these fluxes occur somewhat linearly between sampling days, a linear interpolation between the flux values for the duration of the sample period (30 days) yields average fluxes of DIC and O_2 of 35.8 ± 11.9 and -59.1 ± 18.8 mmol m^{-2} d^{-1}, respectively. An independent DIC flux estimate was made by assessing the deep-water DIC inventory changes seen in Fig. 6. This yields an average increase of 56.2 mmol DIC m^{-2} d^{-1}. This approach yields similar values compared to the above radium method (35.8 mmol DIC m^{-2} d^{-1}), providing support for the flux estimates reported in this study. However, for the further context of this paper, we refer to the radium-based DIC flux estimates.

The time series measurements of nitrate, phosphate and O_2 taken at the Compass Buoy Site during the sampling period (Figs. 4 and 7) show a successive decrease (i.e. consumption) in O_2 at 60 m depth with increases (i.e. production) in both nitrate and phosphate. These rates of consumption and production were used to calculate nitrate (Q_{NO_3}) and phosphate (Q_{PO4}) fluxes from the sediment into the water column of 5.83 ± 1.94 and 0.41 ± 0.29 mmol m^{-2} d^{-1}, respectively. The relative uncertainties in these values differ considerably due to the differing R^2 values of the linear fits (Fig. 7). These nutrient fluxes are summarized in Table 2, and combined with the carbon and oxygen estimates, now present a more complete and quantitative understanding of the return flow of important chemical constituents through the sediment-water interface in Bedford Basin.

4 Discussion

4.1 Application of K_Z measurements

This study demonstrates the utility of water column ^{224}Ra measurements in assessing vertical eddy diffusive coefficients using the simple 1-D diffusion model. Estimates of these coefficients in Bedford Basin will facilitate a number of useful applications in the future. For example, the mixing schemes of physical models in general, are often tuned

BGD
9, 9201–9231, 2012

using a wide range of acceptable mixing coefficients from other published literature. Therefore, observational estimates of coefficients like eddy diffusion on a small scale, like the ones published here, can be very useful in areas where physical models are in place. In this case, the observed diffusivities are useful to validate and improve the vertical mixing scheme of the coastal circulation model for Halifax Harbour (Shan et al., 2011). Furthermore, these estimates can be directly used to fine-tune the vertical eddy diffusivity coefficient used as an input parameter for the random walk process in the recently implemented particle tracking model for Halifax Harbour (Shan and Sheng, 2012).

4.2 Deep-water intrusion

The results here reveal distinct benthic releases of ^{224}Ra, DIC, and nutrients from the sediment, with a corresponding consumption of O_2. However, the evolution in the magnitude of these releases throughout the sampling period points to the occurrence of a significant deep-water intrusion event and provides insight into the effects of such an event on the biogeochemistry of the deep basin (see Fig. 4). The intrusion event appears to have taken place just prior to the initial sampling day (26 October), affecting the entire deep water column (Figs. 2 and 4). At this time, very little gradient in ^{224}Ra is observed and the inferred vertical diffusivity of 25.7 $cm^2 s^{-1}$ is an order of magnitude higher than those calculated for all subsequent profiles in this study (Table 1, Fig. 5). This suggests the presence of enhanced vertical mixing due to the intrusion event. In a recent study by Li and Cai (2011), the same 1-D diffusion model used here is shown to be very sensitive to advection, with the maximum sensitivity occurring when values of K_Z are small, and when using the shorter-lived isotope (i.e. ^{224}Ra). The large relative uncertainty calculated in this instance for K_Z (95 %) likely reflects the sensitivity to small K_Z values and advective signals. The immediate effects of the lateral intrusion are also visible in the biogeochemical data collected on 27 October, namely the abrupt increases in deep water O_2 and particulate organic carbon (POC) levels and corresponding decreases in nutrients (Fig. 4), which indicate the intrusion originated

BGD
9, 9201–9231, 2012

from near the surface. The temperature and salinity properties (Fig. 2) of the deep basin during this time reveal a shift to warmer, more saline water immediately following the event suggesting a shallow, offshore intrusion source, which is consistent with the mechanism described for these intrusion events (Platt, 1975). As a whole, the data in late October indicate a relatively well-mixed deep water column as a result of a lateral intrusion of a water-mass rich in oxygen and POC, and depleted in DIC and nutrients.

The observations throughout the remainder of the sampling period illustrate a re-stabilization of the water column after the intrusion event. The increasing magnitude of the vertical radium gradient (Fig. 5) results in a decrease of calculated K_Z values over time. However, while decreases in the diffusive coefficients will tend to dampen the flux terms (Eqs. 5 and 6), the intensification of the vertical DIC and O_2 gradients, as well as increases in A_0 (Eq. 4), cause the magnitude of the ^{224}Ra, DIC and O_2 fluxes to increase considerably throughout November 2010. These trends can be attributed to the processes that likely occur after the lateral intrusion event, namely the settling of intruded sedimentary material and the biogeochemical reactions that take place within the sediments after deposition. For example, enhanced settling of sedimentary material will result in an enrichment of the particle-reactive parent isotope of ^{224}Ra, ^{228}Thorium, within the sediments, leading to higher ^{224}Ra activities within the pore waters. Similarly, the sharp increase in POC levels at 60 m water depth on 27 October (Fig. 4), followed by its decline one week later, indicate enhanced delivery and settling of POC on the seafloor, eventually fuelling chemical reactions within the sediments.

4.3 Remineralization of organic material

While the calculated fluxes (Table 2) indicate clear sources and sinks of various chemical constituents, the ratios of these fluxes can provide further insight into the origin of the organic material and allow us to speculate about the dominant pathways for remineralization. The observations seen here are consistent with the general notion of benthic respiration as a source of the various chemical constituents released from sediments. Conceptually, the overall net reaction of benthic respiration describes the

BGD
9, 9201–9231, 2012

degradation of organic matter by bacteria within the sediments resulting in both the consumption of O_2, or other electron acceptors, and the formation of DIC (Burdige, 2012). Subsequently, pore waters concentrated in DIC are released along with radium into the water column, while oxygen diffuses into the sediment. The result is a water column flux of DIC away from sediments and an opposing flux of O_2. The effect of these opposing fluxes can be observed in the vertical DIC and O_2 distributions of Bedford Basin (Fig. 6).

According to the concepts first described by Redfield et al. (1963), marine organic matter contains carbon, nitrogen and phosphorus in the average composition of C : N : P=106 : 16 : 1. Therefore, the net oxidation of this material to DIC, NO_3^- and PO_4^{3-} by bacteria within sediments should produce similar ratios in the pore water, with an O_2 : DIC flux across the sediment water interface nearing −1.3 : 1 (Jahnke and Jahnke, 2000). The Bedford Basin observations suggest an O_2 : DIC ratio of $-1.7 \pm 0.7 : 1$ for benthic fluxes, while $DIC : NO_3^- : PO_4^{3-}$ ratios are approximately 87 : 14 : 1 (Table 2). These ratios are a strong indication that bacterial respiration of marine organic matter within the sediments fuels the benthic fluxes into the overlying water column. However, remineralization of organic matter can occur via a number of pathways, involving reactions that result in deviations from the Redfield values, most importantly, denitrification.

The reactions governing the respiration of POM in sediments will depend on the availability of various electron acceptors, with O_2 being most favourable in terms of energy released (Burdige, 2012). Therefore, aerobic oxidation will dominate within the oxygenated layer of sediment directly beneath the sediment-water interface. Beneath this layer, in the absence of O_2, the system will favour the reduction of NO_3^- (denitrification), resulting in a conversion of NO_3^- to elemental N_2, and the production of A_T (Chen and Wang, 1999). Similarly, in the absence of available NO_3^-, the reduction of manganese, iron and sulphate will produce Mn^{2+}, Fe^{2+} and H_2S, respectively, also increasing A_T by varying amounts (Chen and Wang, 1999). However, ignoring the potential burial of S^{-2} as pyrite, upward diffusion of these reduced products into the oxygenated sediment layer will result in their reoxidation, with the corresponding A_T consumed.

BGD
9, 9201–9231, 2012

Therefore, in the presence of strong oxic-anoxic coupling within the sediments, anaerobic processes may play an important role in the respiration of POM, yet O_2 appears to be the dominant oxidant from a net perspective (Burdige, 2012). This may explain the absence of any distinguishable release of A_T from sediments (Fig. 6a), and the apparent dominance of aerobic respiration in producing the observed benthic fluxes, despite a possibly sulfidic character of the sediments beneath the oxygenated layer. In this case, without any direct measurements of the sediment biogeochemistry, the extent of most anaerobic reactions is not fully traceable. For denitrification, however, the reaction produces DIC and A_T while creating an irreversible loss of NO_3^- from the system in the form of N_2, which should, in effect, increase the DIC : NO_3^-, and O_2 : NO_3^- ratios of the observed fluxes. Given the clear increase of nitrate in the deep water column (Fig. 6), the observed NO_3^- related flux ratios compare well to Redfield values. Furthermore, the DIC : NO_3 flux ratio of 6.3 agrees with values previously reported for both deposited and suspended particulate matter in sediment traps in Bedford Basin by Hargrave and Taguchi (1978). Furthermore, no increase in A_T is observed (Fig. 6a). Thus, there is no clear signature of denitrification in the benthic fluxes into the water column observed here.

Considering the short period over which these fluxes are measured (30 days), they constitute substantial additions to the carbon inventory of the basin (Table 2). For example, the Sackville River, on average, delivers only 14.5 mmol DIC m^{-2} d^{-1} to the surface waters of Bedford Basin, which corresponds to less than half of the daily benthic DIC release into the deep water column. Furthermore, when integrating over the 30-day sampling period, the benthic DIC return flux corresponds to approximately 6 % of the annual DIC uptake by primary production in the surface waters (Platt, 1975). While similarly large benthic DIC contributions have been reported previously (Chen and Wang, 1999; Jahnke et al., 2005), they are more common in warmer, shallower shelf environments. In such environments, the euphotic zone is in close proximity to sediments allowing large amounts of organic carbon formed in the surface to reach the sediments, where the organic carbon is respired rapidly. A sediment trap study in the

BGD
9, 9201–9231, 2012

basin by Hargrave and Taguchi (1978) provided annual mean organic carbon sedimentation rates at 60 m depth of 17 mmol C m^{-2} d^{-1}, approximately half of the DIC return flux calculated here during the sampling period. Therefore, even when assuming no long-term burial of sedimented material, our results represent enhanced benthic fluxes compared to those reported by Hargrave and Taguchi (1978). Allochthonous inputs of organic material from rivers and sewage appear to play a very modest role in organic carbon supply to Bedford Basin (Table 2). This is in line with our observed "Redfieldian" release of carbon and nutrients, which in turn points to the respiration of marine organic matter. Furthermore, the modest allochthonous inputs may help sustain the oxic conditions observed in the water column of Bedford Basin throughout the year (Fig. 3) (Hargrave et al., 1976).

POC concentrations increased in the deep waters following the intrusion event in late October (Fig. 4). As argued by Hargrave and Taguchi (1978), an inflow of dense surface water, rich with labile POM and re-suspended sediments, could import the additional organic material necessary to fuel the benthic fluxes we observe. Furthermore, the co-occurrence of the autumn bloom in mid-October (Fig. 4) may have led to organic carbon delivery both vertically via increased particle export from the surface layer and laterally via the deep-water intrusion. Regardless of the delivery mechanism, the observations indicate that an enhanced supply of organic matter becomes available for rapid respiration, which is reflected by the high return fluxes we observe. It is important to note that these fluxes may occur over a short time period and do not necessarily reflect the annual mean fluxes. While the notion of enhanced delivery of POM to the deep basin via lateral intrusion appears reasonable, direct observations of these rare events are needed to completely understand their impact on the chemical budgets, as well as the physical structure, of Bedford Basin.

BGD
9, 9201–9231, 2012

5 Conclusions

Corresponding trends between various hydrochemical measurements point to enhanced benthic respiration and subsequent pore water fluxes of DIC, O_2, and nutrients into the deep water column of Bedford Basin, paralleled by a release of ^{224}Ra. The application of the 1-D diffusion model to near-bottom distributions of ^{224}Ra was useful in understanding the evolving mixing regime of the deep basin following a considerable water-exchange event and yielded vertical eddy diffusivities and fluxes. Fluxes of DIC, nutrients and O_2, consistent in magnitude with Redfield ratios, point to benthic respiration of marine organic matter. Interpolation throughout the 30-day sampling period yields a benthic DIC return flux which constitutes as much as 6 % of the annual primary production in surface waters. This presumed short-term substantial flux is believed to result from enhanced delivery of particulate organic carbon (POC) to deep waters associated with the co-occurrence of the autumn bloom and a deep-water intrusion event.

High seasonal variability in sedimentation rate and relatively high carbon sedimentation rates during fall months have been reported by Hargrave and Taguchi (1978). Long-term Ra and carbon monitoring would be needed in order to gain better understanding of the mixing regimes and benthic fluxes at an annual scale.

Acknowledgements. We thank John Smith, Jeff Spry, Kevin Pauley, the crew of the CCGS Sigma T, as well as Bill Li and the DFO Bedford Basin Plankton Monitoring Program.

References

Berelson, W. M., Hammond, D. E., and Fuller, C.: Radon-222 as a tracer for mixing in the water column and benthic exchange in the Southern California borderland, Earth Planet. Sci. Lett., 61, 41–54, 1982.

Berelson, W. M., Hammond, D. E., and Johnson, K. S.: Benthic fluxes and the cycling of biogenic silica and carbon in two Southern California borderland basins, Geochim. Cosmochim. Acta, 51, 1345–1363, 1987.

BGD

9, 9201–9231, 2012

Burdige, D. J.: 5.09 Estuarine and coastal sediments – coupled biogeochemical cycling, in: Treatise on Estuarine and Coastal Science, Vol. 5, edited by: Wolanski, E. and McLusky, D. S., Academic Press, Waltham, 4, 279–308, 2011.
Burnett, W. C., Bokuniewicz, H., Huettel, M., Moore, W. S., and Taniguchi, M.: Groundwater and pore water inputs to the coastal zone, Biogeochemistry, 66, 3–33, 2003.
Charette, M. A., Gonneea., M. E., Morris., P. J., Statham, P., Fones, G., Planquette, H., Salter, I., and Garabato, A. N.: Radium isotopes as tracers of iron sources fueling a Southern Ocean phytoplankton bloom, Deep-Sea Res. Pt. II, 54, 1989–1998, 2007.
Chen, C.-T. A. and Wang, S.-L.: Carbon, alkalinity and nutrient budgets on the East China Sea continental shelf, J. Geophys. Res., 104, 20675–20686, 1999.
Colbert, S. L. and Hammond, D. E.: Shoreline and seafloor fluxes of water and short-lived Ra isotopes to surface water of San Pedro Bay, CA, Mar. Chem., 108, 1–17, 2008.
Emerson, S., Jahnke, R., and Heggie, D.: Sediment-water exchange in shallow water estuarine sediments, J. Mar. Res., 42, 709–730, 1984.
Fader, G. B. J. and Miller, R. O.: Surficial geology, Halifax Harbour, Nova Scotia, Geol. Surv. Can. Bull., 590, 1–163, 2008.
Fennel, K., Wilkin, J., Levin., J., Moisan, J., O'Reilly, J. O., and Haidvogel, D.: Nitrogen cycling in the Middle Atlantic Bight: Results from a three-dimensional model and implications for the North Atlantic nitrogen budget, Global Biogeochem. Cy., 20, GB3007, doi:10.1029/2005GB002456, 2006.
Fennel, K., Brady, D., DiToro, D., Fulweiler, R. W., Gardner, W. S., Giblin, A., McCarthy, M. J., Rao, A., Seitzinger, S., Thouvenot-Korppoo, M., and Tobias, C.: Modeling denitrification in aquatic sediments, Biogeochemistry, 93, 159–178, 2009.
Hancock, G. J., Webster, I. T., and Stieglitz, T. C.: Horizontal mixing of Great Barrier Reef waters: offshore diffusivity determined from radium isotope distribution, J. Geophys. Res., 111, C12019, doi:10.1029/2006JC003608, 2006.
Hargrave, B. T. and Taguchi, S.: Origin of deposited material sedimented in a Marine Bay, J. Fish. Res. Board Can., 35, 1604–1613, 1978.
Hargrave, B. T., Phillips, G. A., and Taguchi, S.: Sedimentation Measurements in Bedford Basin, 1973–1974, Tech. Rep. Fish. Mar. Serv. Envir., 608, 1–129, 1976.
Huettel, M. and Webster, I. T.: Porewater flow in permeable sediment, in: The Benthic Boundary Layer: Transport Processes and Biogeochemistry, edited by: Boudreau, B. P. and Jorgensen, B. B., Oxford University Press, New York, 144–179, 2001.

BGD
9, 9201–9231, 2012

Jahnke, R. A. and Jahnke, D. B.: Rates of C, N, P and Si recycling and denitrification at the US Mid-Atlantic continental slope depocenter, Deep-Sea Res. Pt. I, 47, 1405–1428, 2000.
Jahnke, R. A., Nelson, J. R., Marinelli, R. L., and Eckman, J. E.: Benthic flux of biogenic elements on the Southerwestern US continental shelf: influence of pore water advective transport and benthic microalgae, Cont. Shelf Res., 20, 109–127, 2000.
Jahnke, R., Richards, M., Nelson, J., Robertson, C., Rao, A., and Jahnke, D.: Organic matter remineralization and porewater exchange rates in permeable South Atlantic Bight continental shelf sediments, Cont. Shelf Res., 25, 1433–1452, 2005.
Johnson, K. M., Willis, K. D., Butler, D. B., Johnson, W. K., and Wong, C. S.: Coulometric total carbon dioxide analysis for marine studies: maximizing the performance of an automated gas extraction system and coulometric detector, Mar. Chem., 44, 167–188, 1993.
Kepkay, P. E, Niven, S. E. H., and Jellett, J. F.: Colloidal organic carbon and phytoplankton speciation during a coastal bloom, J. Plankton Res., 19, 369–389, 1997.
Lettmann, K. A., Riedinger, N., Ramlau, R., Knab, N., Böttcher, M. E., Khalili, A., Wolff, J.-O., and Jørgensen, B. B.: Estimation of biogeochemical rates from concentration profiles: a novel inverse method, Estuar. Coastal Shelf Sci., 100, 26–37, 2012.
Li, W. K. W. and Dickie, P. M.: Monitoring phytoplankton, bacterioplankton, and virioplankton in a coastal inlet (Bedford Basin) by flow cytometry, Cytometry, 44, 236–246, 2001.
Li, C. and Cai, W.-J.: On the calculation of eddy diffusivity in the shelf water from radium isotopes: High sensitivity to advection, J. Mar. Syst., 86, 28–33, 2011.
Men, W., Wang, F., and Liu, G.: ^{224}Ra and its implications in the East China Sea, J. Radioanal. Nucl. Chem., 288, 189–195, 2011.
Moore, W. S.: Radium 228 in the South Atlantic Bight, J. Geophys. Res., 92, 5177–5190, 1987.
Moore, W. S.: Determining coastal mixing rates using radium isotopes, Cont. Shelf Res., 20, 1993–2007, 2000.
Moore, W. S.: Sources and fluxes of submarine groundwater discharge delineated by radium isotopes, Biogeochemistry, 66, 75–93, 2003.
Moore, W. S. and Arnold, R.: Measurement of ^{223}Ra and ^{224}Ra in coastal waters using a delayed coincidence counter, J. Geophys. Res., 101, 1321–1329, 1996.
Moore, W. S. and de Oliveira, J.: Determination of residence time and mixing processes of the Ubatuba, Brazil, inner shelf waters using natural Ra isotopes, Estuar. Coastal Shelf Sci., 76, 512–521, 2008.

BGD
9, 9201–9231, 2012

Moore, W. S., Beck, M., Riedel, T., Rutgers van der Loeff, M., Dellwig, O., Shaw, T. J., Schnetger, B., and Brumsack, H.-J.: Radium-based pore water fluxes of silica, alkalinity, manganese, DOC, and uranium: a decade of studies in the German Wadden Sea, Geochim. Cosmochim. Acta, 75, 6535–6555, 2011.

Platt, T.: Analysis of the importance of spatial and temporal heterogeneity in the estimation of annual production by phytoplankton in a small, enriched, marine basin, J. Exp. Mar. Biol. Ecol., 18, 99–109, 1975.

Platt T., Prakash, A., and Irwin, B.: Phytoplankton nutrients and flushing of inlets on the coast of Nova Scotia, Nat. Can., 99, 253–261, 1972

Punshon, S. and Moore, R. M.: Nitrous oxide production and consumption in a eutrophic coastal embayment, Mar. Chem., 15, 37–51, 2004.

Redfield, A. C., Ketchum, B. H., and Richards, F. A.: The influence of organisms on the composition of sea water, in: Comparative and Descriptive Oceanography, edited by: Hill, M. N., Wiley, New York, 26–77, 1963.

Riddle, A. M. and Lewis, R. E.: Dispersion experiments in UK coastal waters, Estuar. Coastal Shelf Sci., 51, 243–254, 2000.

Shadwick, E. H., Thomas, H., Azetsu-Scott, K., Greenan, B. J. W., Head, E., and Horne, E.: Seasonal variability of dissolved inorganic carbon and surface water pCO_2 in the Scotian Shelf region of the Northwestern Atlantic, Mar. Chem., 124, 23–37, 2011.

Shan, S. and Sheng, J.: Examination of circulation, flushing time, and dispersion in Halifax Harbour of Nova Scotia, Canada, Water Qual., Res. J. Can., under review, 2012.

Shan, S., Sheng, J., and Thompson, K. F.: Simulating the three-dimensional circulation and hydrography of Halifax Harbour using a multi-nested coastal ocean circulation model, Ocean Dynam., 61, 951–976, 2011.

Simmons Jr., G. M.: Importance of submarine groundwater discharge (SGWD) and seawater cycling to material flux across sediment/water interfaces in marine environments., Mar. Ecol. Prog. Ser., 84, 173–184, 1992.

Sun, Y. and Torgersen, T.: Rapid and precise measurement method for adsorbed ^{224}Ra on sediments, Mar. Chem., 61, 163–171, 1998.

Thomas, H., Schiettecatte, L.-S., Suykens, K., Koné, Y. J. M., Shadwick, E. H., Prowe, A. E. F., Bozec, Y., de Baar, H. J. W., and Borges, A. V.: Enhanced ocean carbon storage from anaerobic alkalinity generation in coastal sediments, Biogeosciences, 6, 267–274, doi:10.5194/bg-6-267-2009, 2009.

BGD
9, 9201–9231, 2012

Table 1. Results from ^{224}Ra, carbon and oxygen analyses. Daily results of eddy diffusion coefficients (K_Z), ^{224}Ra activities at the sediment water column interface (A_0), as well as benthic fluxes of ^{224}Ra (Q_{Ra}), DIC (Q_{DIC}) and oxygen (Q_{O_2}) are shown.

Sampling Date	K_Z ($cm^2\,s^{-1}$)	A_0 (dpm $100\,l^{-1}$)	Q_{Ra} (atoms $m^{-2}\,s^{-1}$)	Q_{DIC} ($mmol\,m^{-2}\,d^{-1}$)	Q_{O_2} ($mmol\,m^{-2}\,d^{-1}$)
26 Oct*	25.72 ± 24.32	8.76 ± 1.83	–	–	–
3 Nov	3.29 ± 0.97	11.92 ± 2.24	24.35 ± 41.73	19.88 ± 5.83	−36.51 ± 18.80
17 Nov	1.00 ± 0.26	31.60 ± 8.65	35.52 ± 7.04	–	–
24 Nov	1.93 ± 0.49	16.30 ± 3.74	25.50 ± 16.36	41.46 ± 11.06	−64.71 ± 19.80
2 Dec	1.17 ± 0.31	30.35 ± 8.15	36.91 ± 8.38	58.70 ± 15.51	−42.06 ± 14.01

* Values not included in flux analyses.

BGD
9, 9201–9231, 2012

Table 2. Chemical fluxes in Bedford Basin.

(a) Fluxes of DIC, O_2 and nutrients, with respective flux ratios Fluxes from sediment*		Ratios	mol mol^{-1}
DIC (Q_{DIC}, Radium Method)[a]	35.8 ± 11.9 mmol C m^{-2} day^{-1}	$O_2 : DIC$	-1.7 ± 0.8
DIC (Q_{DIC}, Inventory Method)[b]	56.2 mmol C m^{-2} day^{-1}	$DIC : NO_3^-$	6.2 ± 2.9
Oxygen (O_2) (Q_{O_2})[a]	-59.1 ± 18.8 mmol O_2 m^{-2} day^{-1}	$DIC : PO_4^{3-}$	86.6 ± 66.5
Nitrate (NO_3^-) (Q_{NO_3})[d]	5.83 ± 1.94 mmol N m^{-2} day^{-1}	$O_2 : NO_3^-$[c]	-10.2 ± 1.0
Phosphate (PO_4^{3-}) (Q_{PO_4})[f]	0.41 ± 0.29 mmol P m^{-2} day^{-1}	$O_2 : PO_4^{3-}$[e]	-143.0 ± 87.7
		$NO_3^- : PO_4^{3-}$[g]	14.1 ± 10.8

* During the 30 day sampling period (3 Nov–2 Dec 2010).
[a] Average of linearly interpolated Q_{DIC/O_2} values (Table 1).
[b] See results (Sect. 3.2).
[c] Using slopes of 60 m O_2 and NO_3- time series.
[d] Product of Q_{O_2} and $O_2 : NO_3^-$ ratio.
[e] Using slopes of 60 m O_2 and PO_4^{3-} time series (Fig. 7).
[f] Product of Q_{O_2} and $O_2 : PO_4^{3-}$ ratio.
[g] Using Q_{NO_3} and Q_{PO_4}.

(b) Carbon Fluxes in the Surface Layer	mmol C m^{-2} day^{-1}
DIC Uptake by Primary Production[h]	−50.1
DIC from Sackville River[i]	14.5
OrgC from Sackville River[j]	0.38
OrgC from Sewage Outfall[k]	0.22

[h] Daily average from Platt (1975).
[i] Using riverine DIC endmember (601 µmol kg^{-1}, Shadwick et al., 2011), average river discharge (1.5×10^8 m^3 yr^{-1}, Kepkay et al., 1997), and 17 km^2 for surface area of basin.
[j] From Hargrave and Taguchi (1978).
[k] Converted from CBOD data provided by Mill Cove Wastewater Treatment Plant (WWTP).

BGD
9, 9201–9231, 2012

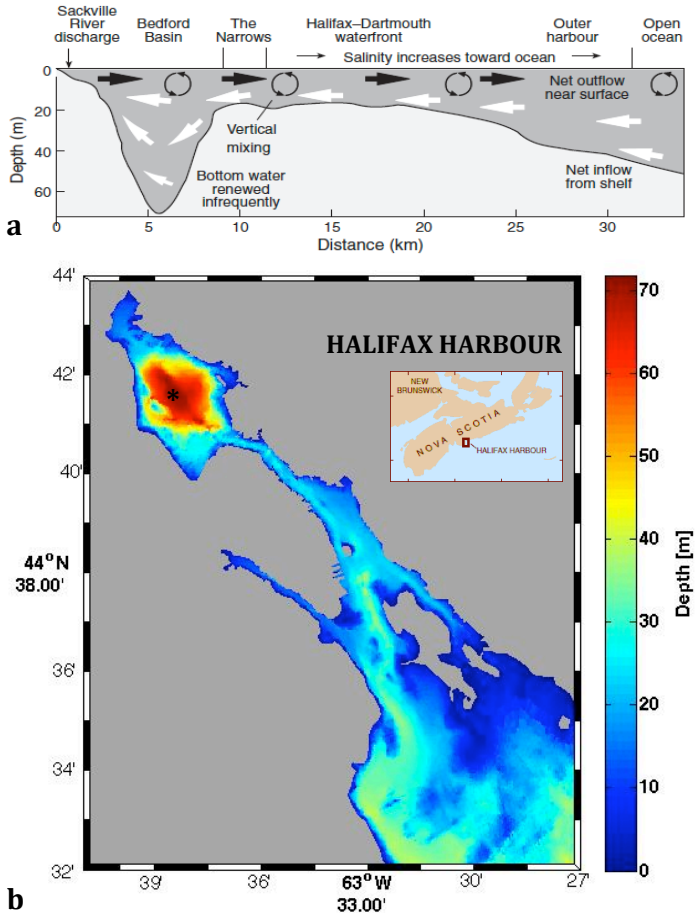

Fig. 1. (a) Schematic cross-section of Halifax Harbour (with permission from Fader and Miller, 2008). **(b)** Bathymetric map of Halifax Harbour, showing the Compass Buoy Site (*) in Bedford Basin.

BGD
9, 9201–9231, 2012


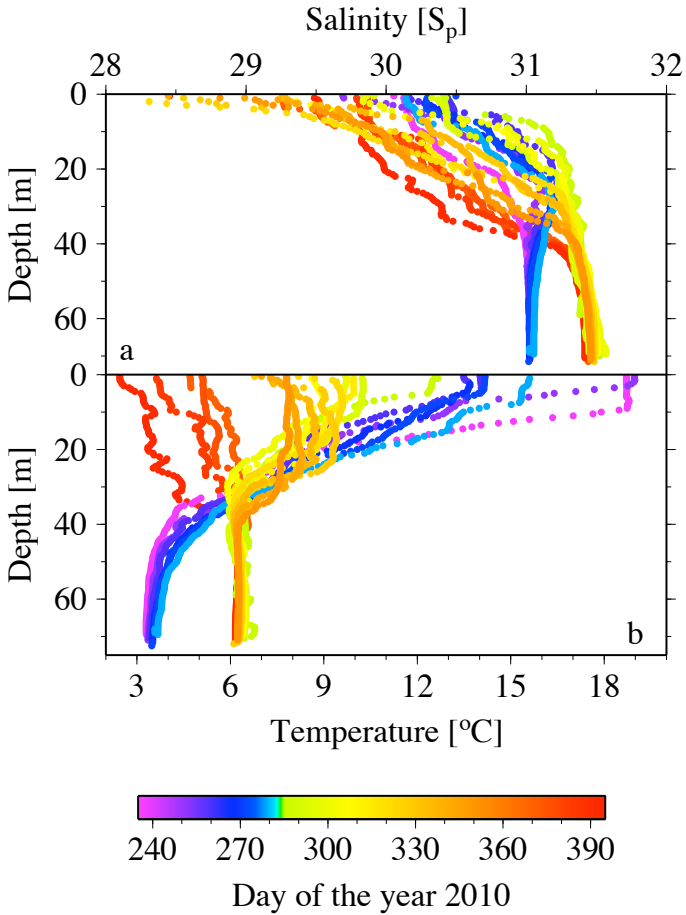

Fig. 2. Weekly vertical profiles of salinity (S_p) **(a)** and temperature **(b)** from August 2010 (day 237)–January 2011 (day 391). The colorbar has been adjusted at day 282 (9 October) in order to better illustrate the abrupt changes in the deep waters around that day.

BGD
9, 9201–9231, 2012

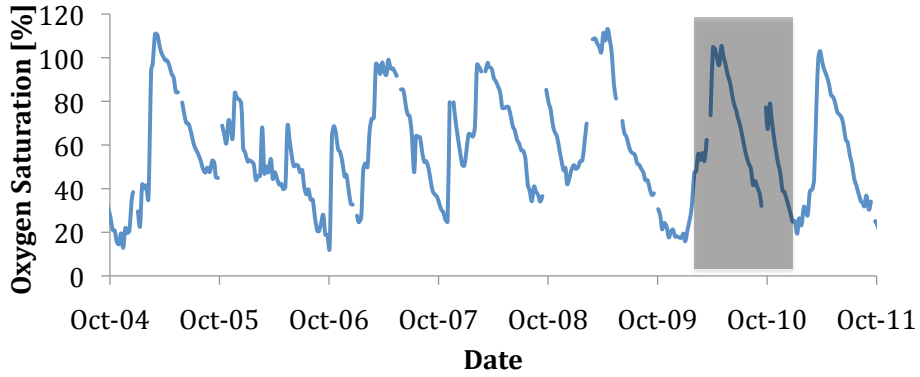

Fig. 3. Deep-water (60 m) oxygen saturation time-series at the Compass Buoy Site in Bedford Basin. An abrupt increase indicates a deep-water mixing event. Two distinct events are shown to occur in 2010 (shaded box).

BGD
9, 9201–9231, 2012

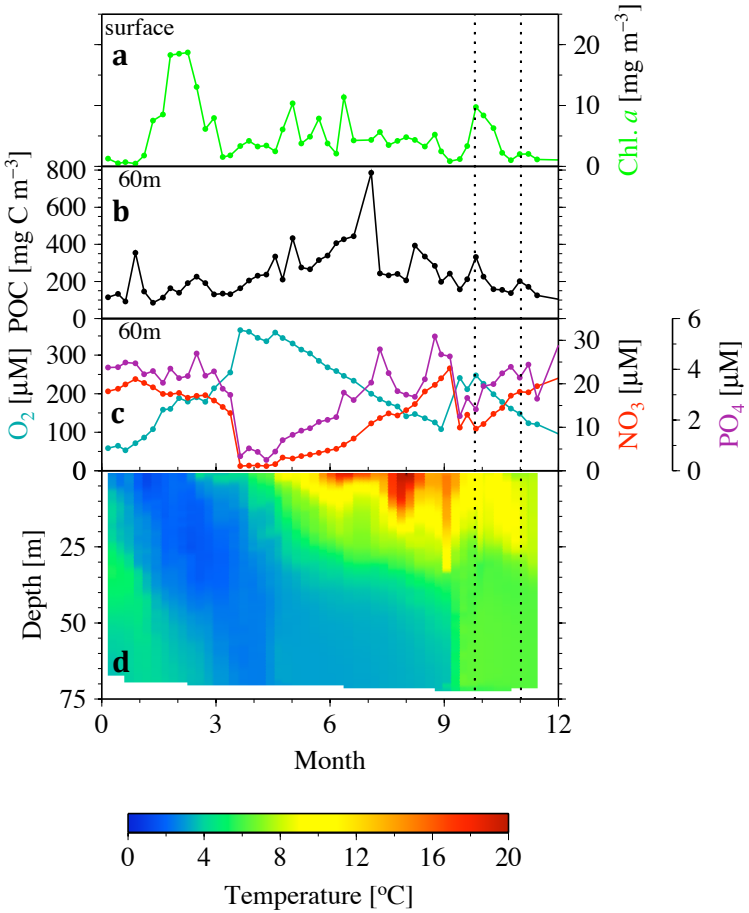

Fig. 4. Time series of surface Chl *a* **(a)**, deep-water particulate organic carbon (POC) **(b)**, deep-water oxygen and nutrients **(c)**, and temperature depth profiles **(d)** in Bedford Basin during 2010. Black dashed lines indicate the sampling period of the study.

BGD
9, 9201–9231, 2012

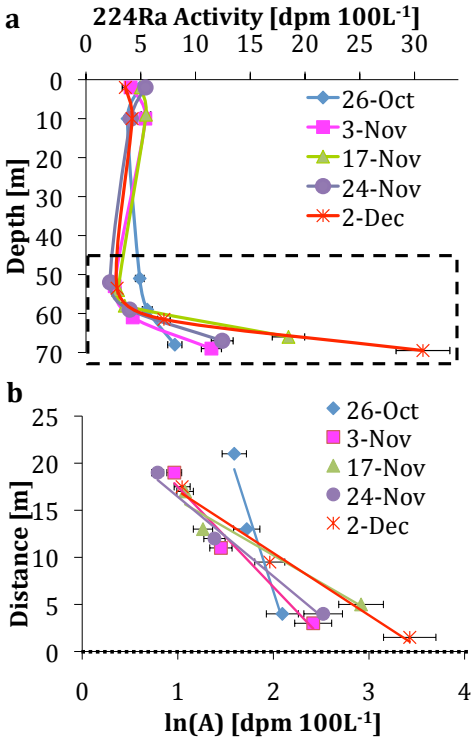

Fig. 5. (a) Vertical profiles of ^{224}Radium. Black dashed box indicates deep-water samples used in 1-D diffusive model. **(b)** Natural log (ln) transformations of ^{224}Ra activity plotted as a function of distance from the sediment surface (dotted line). Each daily set of points is fit with a least-squares regression used to estimate mixing rates (K_Z) and interface activities (A_0). The different characteristics of the 26-Oct plot relative to all other days represents the different mixing regime during this period.

BGD
9, 9201–9231, 2012

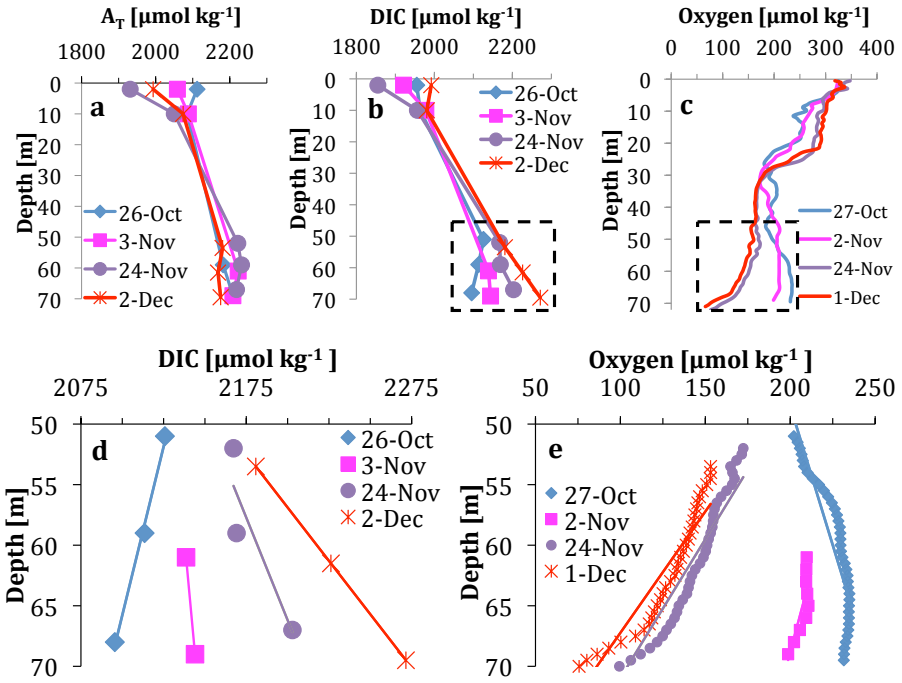

Fig. 6. Top: Vertical profiles of A_T **(a)**, DIC **(b)**, and O_2 **(c)** in Bedford Basin. Black dashed boxes indicate deep-water samples shown in bottom panels. Bottom: Vertical profiles of DIC **(d)** and O_2 **(e)** in deep waters with least-squares regression lines indicating gradients. Note: The DIC decrease with distance from the sediments indicates a negative flux.

BGD
9, 9201–9231, 2012

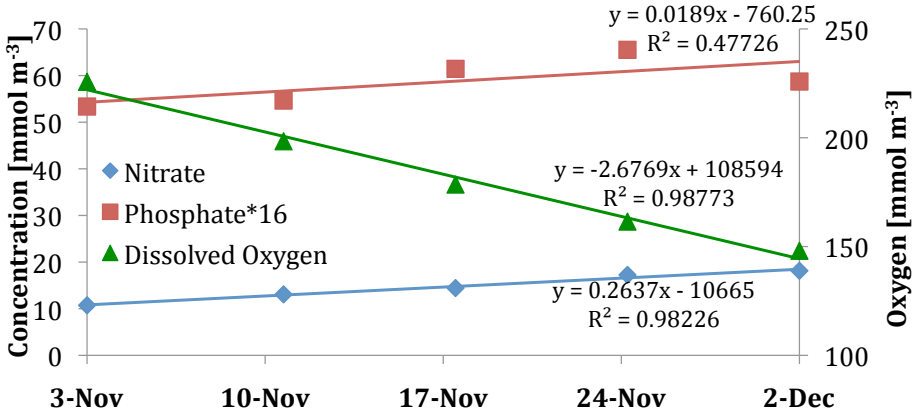

Fig. 7. Time-series measurements at 60 m in Bedford Basin during the sampling period (as shown in Fig. 4). Rates of change used to calculate $O_2 : NO_3^-$ and $O_2 : PO_4^{3-}$ ratios are shown as the slopes of the linear regression curves. The R^2 values represent the quality of the fit, which largely affects the uncertainties in the final flux estimates. Note that phosphate regression coefficients are from the original data rather than "Phosphate*16", which is shown to better illustrate the parallel nature of the nitrate and phosphate slopes.

BGD
9, 9201–9231, 2012